ARTICLE

doi:10.1016/j.ymthe.2003.08.016

Optimization of Adenoviral Vectors to Direct Highly Amplified Prostate-Specific Expression for Imaging and Gene Therapy

Makoto Sato,[1] Mai Johnson,[1] Liqun Zhang,[2] Baohui Zhang,[1] Kim Le,[2] Sanjiv S. Gambhir,[3]* Michael Carey,[2,3] and Lily Wu[1,3,†]

[1]*Department of Urology,* [3]*Crump Institute of Molecular Imaging and Department of Molecular and Medical Pharmacology, and* [2]*Department of Biological Chemistry, University of California at Los Angeles School of Medicine, Los Angeles, California 90095*

**Present address: Department of Radiology and Bio-X Program, Stanford University, Stanford, CA.*

[†]*To whom correspondence and reprint requests should be addressed. Fax: (310) 206-5343. E-mail: LWu@mednet.ucla.edu.*

Gene expression-based imaging coupled to gene therapy will permit the prediction of therapeutic outcome. A significant challenge for successful gene therapy is to achieve a high-level of specific gene expression; however, tissue-specific promoters are weak. We postulate that if the weak activity of tissue-specific promoters can be amplified to the levels of strong viral promoters, which have been successful in preclinical scenarios, while retaining specificity, the therapeutic index of gene therapy can be greatly augmented. With this in mind, we developed a two-step transcriptional activation (TSTA) system. In this two-tiered system, a modified prostate-specific antigen promoter was employed to drive a potent synthetic transcriptional activator, GAL4-VP2. This, in turn, activated the expression of a GAL4-dependent reporter or therapeutic gene. Here we demonstrate that recombinant adenoviral vectors (Ads) in which we have incorporated prostate-targeted TSTA expression cassettes retain cell specificity and androgen responsiveness in cell culture and in animal models, as measured by noninvasive optical bioluminescence imaging. We investigated the mechanism of TSTA in different adenoviral configurations. In one configuration, both the activator and the reporter components are inserted into a single Ad (AdTSTA-FL). The activity of AdTSTA-FL exceeds that of a cytomegalovirus promoter-driven vector (AdCMV-FL), while maintaining tissue specificity. When the activator and reporter components are placed in two separate Ads, androgen induction is more robust than for the single AdTSTA-FL. Based on these findings, we hope to refine the TSTA Ads further to improve the efficacy and safety of prostate cancer gene therapy.

Key Words: prostate-specific expression, two-tiered amplification, androgen regulation, adenoviral vector, optical imaging

INTRODUCTION

Metastatic and recurrent hormonal refractory prostate cancer (HRPC) account for an estimated loss of one life every 17 minutes in the United States [1]. Androgen ablation is the main treatment for advanced disease and can induce an initial remission and achieve symptomatic improvement in 80–90% of patients [2–4]. However, progression to HRPC is inevitable even in the absence of circulating androgen. Currently, there is no effective treatment for HRPC, and median survival is approximately 12 months. Gene-based therapy is a promising possibility for HRPC [5,6]. However, an important prerequisite for developing a safe and effective therapy is to achieve high levels of prostate-specific gene expression *in vivo* [6].

The use of tissue-specific promoters to express transgenes is an attractive approach that is particularly suitable for prostatic tissue, because it is one of the organs other than the pancreas and breast that expresses an unusually high number of unique genes. A survey of the Cancer Genome Anatomy Project database published by the National Cancer Institute (http://www.ncbi.nlm.nih.gov/ncicgap/) lists more than 2000 prostate-specific genes, although the majority of them are not fully characterized at this time. Many prostate-specific genes, including pros-

1525-0016/03 $30.00

tate-specific antigen (PSA) and prostate-specific membrane antigen, are well characterized [7–12]. The PSA gene is regulated by testosterone (T) and dihydrotestosterone (DHT), which bind androgen receptor (AR). The ligand-bound AR binds directly to sites within the PSA promoter and enhancer, thus activating PSA gene expression [7,10,11]. Clinical findings indicate that AR and PSA are expressed in all stages of prostate cancer and in distant metastases, even after androgen-deprivation therapy [13–16]. Currently, serum PSA measurements remain the most reliable means to detect recurrent HRPC [17]. Numerous studies support the likelihood that the AR pathway is still functioning in HRPC at castrated levels of DHT and T. Several mechanisms have been proposed to facilitate AR function under androgen-deprived conditions [6,18], such as AR overexpression [19]; increased expression of the nuclear receptor transcriptional coactivators, SRC-1 and SRC-2 [20]; AR mutations that confer expanded ligand specificity [21]; or cross talk between other signaling cascades and AR pathways [22].

We were interested in generating systems for delivery of therapeutic and imaging genes to prostate cancer. We designed our systems around the PSA promoter because of its ability to function in early androgen-dependent prostate cancer and in advanced-stage HRPC [23] and metastasis. Although the native PSA regulatory elements confer tissue selectivity, their activity is too weak to mediate efficient vector-based gene expression *in vivo* [6]. Therefore, we have undertaken two strategies to augment the activity of the PSA promoter/enhancer, while maintaining its specificity. First, the upstream enhancer core of PSA was duplicated in a construct designated PSE-BC, which achieved 20-fold enhancement of activity compared to the native PSA enhancer and promoter construct [24,25]. An adenoviral vector (Ad) bearing this PSE-BC promoter-driven firefly luciferase (FL) gene was able to achieve targeted expression in distant metastatic prostate cancer cells in living mice [26]. In a second approach, we employed a two-step transcriptional amplification (TSTA) system both to elevate and to modulate the activity of the PSA enhancer/promoter over a 1000-fold range [27,28]. In this two-tiered system illustrated in Fig. 1a, the PSA regulatory region was employed to express the potent synthetic transcription activator, GAL4-VP2, which in turn activates a GAL4-responsive reporter. In tissue culture transfection studies, optimal TSTA constructs displayed levels of activity significantly higher than the cytomegalovirus immediate early promoter (CMV), while maintaining prostate cell specificity and ligand responsiveness [27,28].

Imaging of vector-mediated transgene expression provides a critical assessment of the *in vivo* capabilities of targeted gene transfer. Rapid advances in imaging technology have allowed repetitive monitoring of the location, magnitude, and kinetics of reporter gene expression in small living animals [29–31]. Optical bioluminescence imaging (BLI) is particularly suitable for small animal studies, with the distinct advantage of low background signal, rapid scanning time, and low cost in comparison to radionuclide imaging. The *in vivo* expression of the popular FL reporter gene can be monitored by a highly sensitive cooled charge-coupled device (CCD) camera after the administration of the relatively nontoxic d-luciferin substrate in living animals [32,33]. Because imaging can provide real-time information on *in vivo* biological processes, the BLI technology was used to monitor estro-

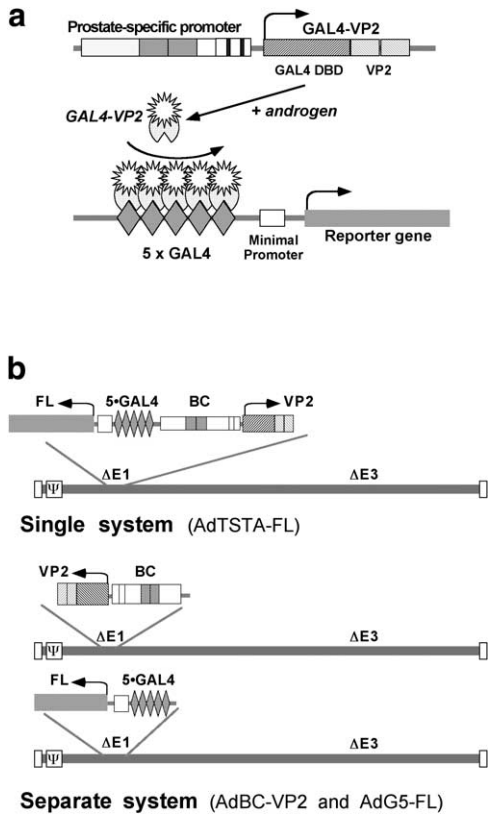

FIG. 1. Schematic representation of TSTA system. (a) Illustration of the two-step transcriptional activation process. In the first step, GAL4-VP2 activator proteins (fusion of GAL4 DNA binding domain and two copies of the VP16 transactivation domain) are expressed under the control of a prostate-specific promoter (an augmented PSA promoter, PSE-BC), which is activated by androgen. In the second step, GAL4-VP2 binds to a GAL4-responsive promoter and activates the expression of the FL reporter gene. (b) The two different TSTA configurations in Ad. In the single TSTA Ad (AdTSTA-FL), both activator and reporter are inserted into the E1 region of the same Ad in a head-to-head orientation. In the separate TSTA Ads (AdBC-VP2 and AdG5-FL), activator and reporter components are incorporated into the E1 region of two separate Ads with the transcription oriented toward the left end of the viral genome. BC is the abbreviation of the PSE-BC prostate-specific promoter [25]. ψ denotes the packaging signal of adenovirus and open rectangles at both termini denote inverted terminal repeats of the viral genome.

doi:10.1016/j.ymthe.2003.08.016

gen receptor function under physiological conditions and during pharmacological intervention [34].

To assess the potential of the TSTA system in gene therapy applications, we incorporated the system into an Ad, which is an efficient *in vivo* gene delivery vehicle. The purpose of this study was to investigate the *in vivo* specificity of and the parameters necessary to achieve optimal regulation of the TSTA system in different Ad configurations. In the AdTSTA-FL construct, the activator and reporter component were inserted into the Ad in a divergently linked head-to-head configuration. Alternatively, two Ads that separately express the GAL4-responsive FL and the PSE-BC-regulated GAL4-VP2 activator were also generated. We analyzed the prostate-specific expression and androgen regulation of the separate TSTA Ads in comparison to the single AdTSTA-FL *in vitro* and *in vivo*. We found that separate Ads elicited a more robust response to androgen versus the single Ad.

RESULTS

Generation of Adenovirus Vectors Containing the TSTA System

The TSTA system is schematically represented in Fig. 1a. We previously determined the combination of activator and reporter plasmid TSTA constructs that achieves the highest levels of activity in prostate cancer cells using transfection studies [28]. Based on these results, we generated TSTA Ads, utilizing the bacterial recombination AdEasy methodology [35]. The activator is composed of an augmented prostate-specific PSE-BC promoter/enhancer [25] controlling the expression of the chimeric activator protein, GAL4-VP2 (the GAL4 DNA-binding domain fused to two tandem repeats of the herpes simplex virus VP16 activation domain) [28]. The reporter component consists of five repeats of the 17-bp GAL4 binding sites positioned upstream of a minimal promoter containing the adenovirus E4 gene TATA box driving FL. We inserted the activator (BC-VP2) and reporter (G5-FL) components linked in a divergent head-to-head orientation into the E1 region of the Ad, resulting in the AdTSTA-FL vector (Fig. 1b). We also constructed two Ads, designated AdBC-VP2 and AdG5-FL, which harbor the BC-VP2 activator and the G5-FL reporter, respectively (Fig. 1b).

Specificity of the TSTA Vectors

We evaluated the capability of AdTSTA-FL to direct prostate-specific expression by infecting a variety of cell lines derived from different tissues. Human serotype 5 Ad exhibits wide cell-type viral tropism. However, the susceptibility of a cell line to Ad infection is modulated by the cell surface expression of coxsackievirus and adenovirus receptor (CAR) [36,37] and αv integrins [38]. Thus, a measurement of infectivity in different cell lines is needed to assess the activity of AdTSTA-FL. Initially, we determined relative infectivity of different cells by normalization to the activity of AdCMV-FL, in which the FL expression is driven by the constitutively active CMV promoter. Our view was that similar pfu (plaque-forming unit) amounts of AdTSTA-FL and AdCMV-FL should display similar infectivity. Thus, differences in the activity of AdCMV-FL in different lines would represent a standard for normalizing infectivity of AdTSTA-FL. However, two findings alerted us to the potential inaccuracy of this measurement: (1) a 3- to 4-fold androgen induction was noted in the AdCMV-FL-infected prostate cell lines (data not shown) and (2) a greater than 30-fold difference in activity was observed between the most and the least active cell lines infected with equivalent doses of AdCMV-FL (data not shown). Discrepancy between luciferase activity and physical viral DNA measurement mediated by AdCMV-luc in different cell types has been reported [39]. An ideal assay to measure infectivity is not available.

In this study we elected to use the viral DNA uptake in the cells as a measurement of infectivity. We harvested the internalized viral DNA from infected cells and quantified the FL DNA by real-time PCR. We determined the infectivities of LNCaP and LAPC-4 (prostate carcinoma), H157 and A549 (lung cancer), MCF-7 (breast carcinoma), HepG2 (liver cancer), and HeLa (cervical carcinoma) cell lines by this viral DNA uptake approach. Among the panel of cell lines that we tested, HeLa cells were the least susceptible to infection and their infectivity was designated as 1. The infectivities of LNCaP, H157, A549, MCF7, LAPC-4, and HepG2 cells were 1.7-, 1.6-, 1.5-, 1.3-, 1.1-, and 1.1-fold higher than that of HeLa cells, respectively. Differential CAR expression in different stages of prostate carcinoma [40] might contribute to the enhanced infection in LNCaP cells.

We evaluated the activity of AdTSTA-FL in several prostate cancer cell lines, including two androgen-responsive cell lines (LNCaP and LAPC-4 [41]) and two AR-negative lines (DU145 and PC-3). Infection was carried out at a calculated AdTSTA-FL dosage of 1 infectious unit (pfu) per cell (m.o.i. 1). The normalized FL activity in LAPC-4 was 4.4-fold lower than LNCaP (see Fig. 5b and data not shown). Conversely, the FL activity in AR-negative prostate cancer lines was negligible (nearly 500-fold lower than in LNCaP cells, data not shown). For simplicity, we compared the normalized FL activities to that of the LNCaP cell line, set at 100% (Fig. 2a). The activity in A549, H157, HepG2, HeLa, and MCF7 cells was 290-, 1200-, 4500-, 6000-, and 20,000-fold lower than in LNCaP cells, respectively (Fig. 2a). The FL activity in nonprostate cell lines and AR-negative prostate cancer lines was not induced by androgen (data not shown). We also observed consistent diminished cell-specific expression in infections. At higher m.o.i. the cell specificity became less apparent due to higher androgen-independent or basal activity, an effect that we do not completely understand (data not shown). For example, AdTSTA-FL-mediated activity in HeLa cells at m.o.i. 10 was 660-fold lower than in

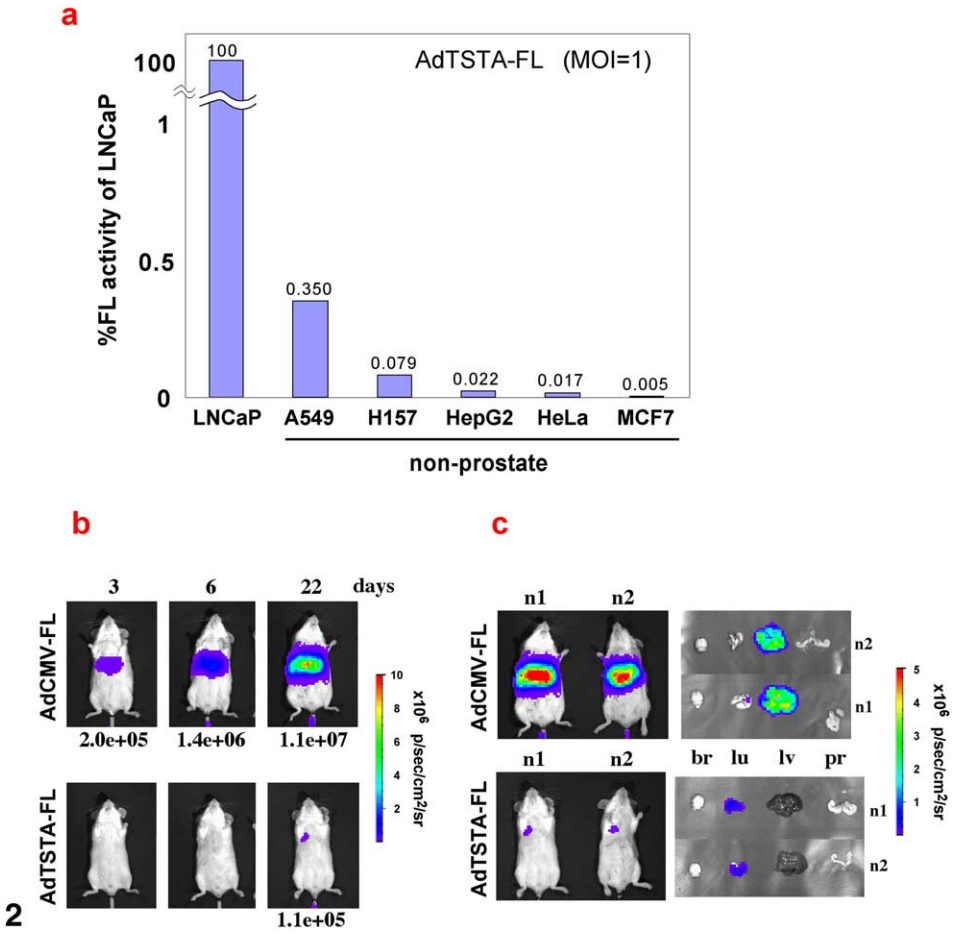

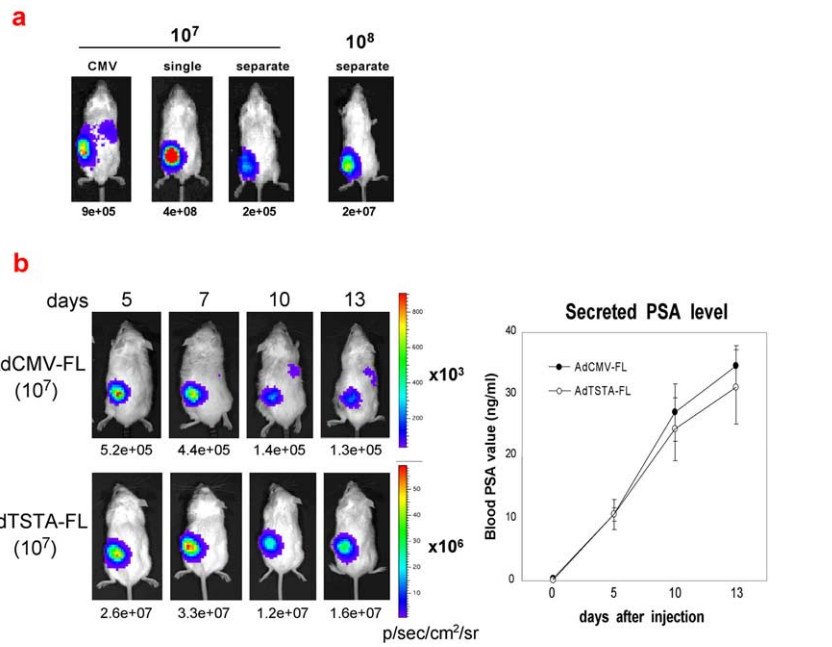

doi:10.1016/j.ymthe.2003.08.016

LNCaP cells, compared to 6000-fold at m.o.i. 1 (data not shown; see Discussion).

We next investigated the specificity of the single AdTSTA-FL *in vivo*. We compared its activity to that of AdCMV-FL, because vector DNA quantitation studies in animals are less well controlled. We employed CCD imaging to monitor *in vivo* expression over a 22-day period. Fig. 2b illustrates the optical imaging profiles of animals that received systemic administration of AdTSTA-FL or AdCMV-FL. A robust signal emanating from the midsection of mice injected with AdCMV-FL via the tail vein was seen as early as 3 days postinjection, which we determined was due to efficient liver transduction as assessed by imaging of isolated organs (Figs. 2b and 2c). In contrast, the AdTSTA-FL-injected animals did not have detectable signals until a late time point (day 22), which signals then appeared in the lung (Figs. 2b and 2c); however, this signal is more than 3 orders of magnitude lower than tumor-directed expression (see Fig. 3). The absence of optical signal in the prostate after tail vein injection of AdTSTA-FL is unclear at this time. However, limitations of *in vivo* Ad distribution that result in low gene transfer to organs other than mouse liver have been well documented [42]. We expand on these issues under Discussion.

We next evaluated intratumoral activity mediated by both single and separate TSTA Ads in LAPC-4 xenografts, which were derived from a lymph node metastatic lesion from a patient [41]. LAPC-4 expresses PSA and AR and exhibits androgen-responsive gene expression and growth. Fig. 3a shows that intratumoral injection of 10^7 pfu of the single AdTSTA-FL resulted in a robust signal at 4 days postinjection, compared to AdCMV-FL. In a cohort of four animals, the average activity of AdTSTA-FL was 110-fold higher than that seen with AdCMV-FL ($P = 0.06$).

Cancer-specific gene therapy based on activation of a toxic gene by the Cre/lox recombination system delivered by separate two Ads has been reported to work in animals [43,44]. However, *in vivo* transduction of the two paired TSTA Ads, AdBC-VP2 and AdG5-FL, into the same cell, is anticipated to be less effective than delivery of a single vector containing both elements. Thus, it is not surprising that injection of 10^7 pfu of each of the two Ads resulted in lower optical signal (2×10^5 photons/s/cm^2/sr) versus single Ad (4×10^8 photons/s/cm^2/sr). When the dose of the two paired TSTA Ads was increased to 10^8 pfu each, expression level (2×10^7 photons/s/cm^2/sr) higher than that of 10^7 pfu of AdCMV-FL (9×10^5 photons/s/cm^2/sr) was achieved (Fig. 3a). However, this magnitude of activity is still lower than can be achieved by 10^7 pfu of AdTSTA-FL (4×10^8 photons/s/cm^2/sr).

We examined the kinetics of expression after intratumoral delivery of 10^7 pfu of AdCMV-FL and AdTSTA-FL into LAPC-9 tumors. The LAPC-9 xenograft expresses AR and PSA and was derived from a bone metastasis [41]. Sequential optical images between 5 and 13 days postviral injection were recorded (Fig. 3b). The TSTA vector displayed 50- to 100-fold higher levels of FL activity than the AdCMV-FL during this period (Fig. 3b). The increasing serum PSA levels in both groups likely reflect the increase in tumor mass over the duration of the time course (Fig. 3b, right). However, despite the consistent increase in serum PSA levels the intratumoral FL signals gradually decayed after day 7 in both the AdCMV and the AdTSTA cohorts (Fig. 3b) due to the transient nature of Ad-mediated gene expression. The LAPC-9 tumors, like the LAPC-4 tumors, show a propensity for vector leakage into systemic circulation. However, we consistently observed a greater magnitude of leakage in LAPC-4 tumors, which was manifested as prominent signals in the liver after intratumoral injection of AdCMV-FL [26]. Because both vectors (TSTA and CMV) are serotype 5 adenovirus with the same deletion of the E1 and E3 genes, their biodistribution in mice should not differ. Intratumoral injection of AdTSTA-FL should result in the same extent of vector leakage as AdCMV-FL. However, no detectable liver signal was observed after intratumoral injection of AdTSTA-FL.

FIG. 2. Cell specificity of the TSTA Ad. (a) *In vitro* cell specificity of AdTSTA-FL. The prostate cell line LNCaP and nonprostate cell lines were infected with AdTSTA-FL at m.o.i. 1. Cells were harvested and subjected to an FL assay 48 h after infection. FL activity was normalized to cell numbers and infectivity of each cell line as assayed by real-time PCR (see Materials and Methods). FL activity was plotted for each cell line using LNCaP (an androgen-responsive prostate carcinoma line) as a normalization standard, set at 100%. The activities in nonprostate cell lines are more than 290-fold lower than in LNCaP. (b) *In vivo* tissue specificity of AdTSTA-FL. 10^7 pfu (plaque-forming units = infectious units) of Ad was injected into naïve mice via the tail vein and FL expression was sequentially monitored by optical imaging at days 3, 6, and 22. Robust liver signals were noted in the AdCMV-FL-injected animals starting at day 3 and increasing from that point onward. The AdTSTA-FL-injected animals remained transcriptionally silent until day 22, when a weak signal was noted in the lung. Numbers below the images are the maximal activities in the region of interest as photons (p) acquired per second per square centimeter per steridan (sr). (c) Optical activities in the isolated organs. Two additional animals (n1 and n2) from the AdCMV-FL- or AdTSTA-FL-injected group were sacrificed at day 22, and the isolated organs were reimaged. The liver is the predominant site of expression in AdCMV-FL-injected animals. Low level of expression in the lung was observed in the AdTSTA-FL-injected animals (br, brain; lu, lung; lv, liver; and pr, prostate).

FIG. 3. *In vivo* FL expression mediated by single and separate TSTA Ads in LAPC-4 xenografts and prostates. (a) Optical signals after injections of the respective Ads in LAPC-4 tumors. 10^7 or 10^8 pfu of Ads (as specified) was injected. The injection of separate Ads denotes the coadministration of both AdBC-VP2 and AdG5-FL at the specified dosage. CCD images of representative animals analyzed at 4 days postinjection were shown. (b) Kinetics of FL expression in LAPC-9 tumors. 10^7 pfu of AdCMV-FL or AdTSTA-FL was injected intratumorally. Optical signals were monitored on the specified days after viral injection. The number below each image represents the maximal signal over the tumor. The graph on the right represents the averaged serum PSA level measured in the animals at the specified days post-viral injection.

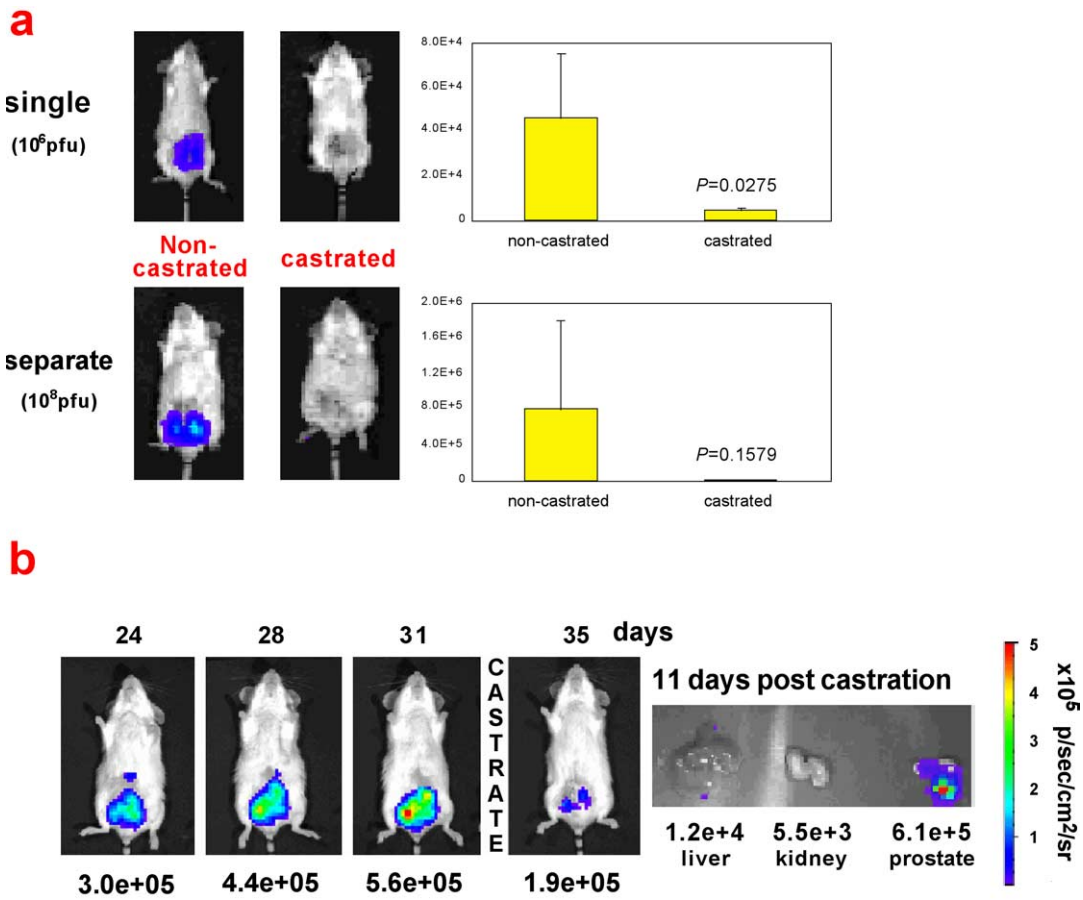

FIG. 4. Intraprostatic signals in intact and castrated animals. (a) AdTSTA-FL (10^6 pfu) or AdBC-VP2 and AdG5-FL (10^8 pfu each) were injected into the prostate of intact and castrated male SCID (7-days postcastration). The images were taken 4 days after viral injection. In each group, n is ≥ 3 animals. The averages and standard errors are plotted on the right. The FL signals in the castrated animals were 4.7×10^3 and 9.6×10^3 with single and separate TSTA Ad, respectively. The significance between intact and castrated animals is denoted in each graph as the P value. (b) The FL signal mediated by AdTSTA-FL in the same animal before and after castration. 10^7 pfu of AdTSTA-FL was injected into prostate in intact SCID mice. Days post-intraprostatic viral injection are indicated above the mouse images. The animal was castrated at day 31 and reimaged at day 35 (4 days postcastration). The animal was sacrificed at 11 days postcastration (day 42). The prostate gland was the predominant site of expression. The optical activity is specified below each image.

This finding supports our view that the prostate specificity of TSTA is able to prevent expression of FL in the liver.

Androgen Regulation of the TSTA Ads

To determine if TSTA Ads respond to androgen regulation *in vivo* we assessed FL expression in the prostates of intact and castrated male SCID mice (Fig. 4). We injected 10^6 pfu of AdTSTA-FL or 10^8 pfu each of AdBC-VP2 and AdG5-FL into the prostate glands of cohorts of either intact male mice or mice castrated 7 days prior to injection (androgen-deprived group). The intact males infected with the single- or two-virus TSTA vectors displayed significant optical signals compared to the castrated mice. We conclude that both vector systems are responding to androgen depletion *in vivo* (Fig. 4a). The FL expression level of a 100-fold higher dose of the separate TSTA Ads was 20-fold greater than that of the single AdTSTA-FL (Fig. 4a, graphs). We also observed androgen regulation of AdTSTA-FL in the prostate gland when castration was performed 30 days postinjection, after FL expression had stabilized. In this case a 3-fold drop in expression was observed 3 days after castration (Fig. 4b).

To investigate androgen regulation of the TSTA Ads in more detail, we employed cell culture infection studies, in which the concentration of androgen and its antagonists could be carefully manipulated. We infected two androgen-dependent prostate cancer cell lines, LNCaP and LAPC-4, with TSTA Ads at different m.o.i. and androgen concentrations. Androgen levels in the medium were manipulated by adding R1881 (methylenetrienolone), a synthetic androgen that is more stable than DHT under culture conditions. The antagonist Casodex was used to minimize residual androgen activity in the charcoal-

doi:10.1016/j.ymthe.2003.08.016

stripped serum because even low androgen levels activate the highly sensitive TSTA system. Both the activator and the reporter TSTA components are required to generate detectable FL in the two-virus system (Fig. 5a). Additionally, androgen stimulated the FL activity for both the separate and the single TSTA Ads, with the highest activity observed between 1 and 10 nM R1881. In Fig. 5b, AdTSTA-FL demonstrates a clear m.o.i.- and R1881-dependent increase in FL activity. In the presence of 1 nM R1881, activity increased 27-fold from m.o.i. 0.1 to m.o.i. 1 in LNCaP cells and 96-fold from m.o.i. 1 to m.o.i. 10 in LAPC-4 cells.

We also quantitated the androgen response of TSTA Ads by calculating the fold induction, based on the ratio of the highest activity at 10 nM R1881 over the basal activity in the presence of Casodex. Both separate and single TSTA Ads exhibited high levels of androgen induction in LNCaP and LAPC-4 cells. The androgen induction observed in infections at m.o.i. 1 and 5 of separate Ads were 672- and 915-fold, respectively, in LNCaP cells, and 52- and 67-fold, respectively, in LAPC-4 cells. The androgen induction mediated by the single AdTSTA-FL was 117- and 101-fold at m.o.i. 1 and 5 in LNCaP cells, respectively, and 35- and 24-fold in LAPC-4 cells at m.o.i. 1 and 5, respectively. The single AdTSTA-FL displayed diminished androgen inducibility compared to separate TSTA Ads. This point is illustrated in Fig. 5c by a plot of the relative induction ratio of separate Ads to single AdTSTA-FL in LNCaP and LAPC-4 cells at the two different m.o.i. The lower inducibility of AdTSTA-FL is not due to a lower maximal activity, but to a higher basal activity (in the presence of Casodex). Because this higher basal activity could potentially contribute to reduced specificity, we investigated the activation mechanism of TSTA Ads in more detail.

Investigating the Activation Mechanism in Single and Separate TSTA Ads

To investigate the mechanism responsible for differences in androgen induction, we analyzed FL activity and activator protein expression profiles over a wide range of infection ratios. LNCaP cells were infected with AdTSTA-FL at m.o.i. of 50, 16.7, 5.6, 1.9, 0.62, and 0.21 (threefold serial dilutions). For the separate system, we added AdBC-VP2 and AdG5-FL at the indicated m.o.i. to generate levels of activator and reporter gene delivery equivalent to those in the single AdTSTA-FL infections. We demonstrated by Southern blotting that equal m.o.i. of AdTSTA-FL and AdBC-VP2 led to equivalent amounts of vector delivery (data not shown). We then examined FL activity and activator expression 48 h postinfection, as shown in Fig. 6. It is difficult to compare directly the levels of FL activity of single and separate Ad infections, especially at low m.o.i., due to the limited codelivery. However, both systems exhibited m.o.i.-dependent increases in activity as indicated in earlier figures. We observed a saturation of activity in both single and separate TSTA vectors. Overall, the magnitude of FL activity corresponded very well with the level of GAL4-VP2 expression measured by Western blotting. In the single AdTSTA-FL infections, the GAL4-VP2 expression reached a maximum at m.o.i. 16.7. We did not observe a plateau of activator expression in the separate TSTA infections at the range of m.o.i. tested. A surprising finding was that at each m.o.i., the activator expression in the single AdTSTA-FL was considerably higher than that mediated by the AdBC-VP2 in the separate system, despite comparable levels of activator (BC-VP2) gene delivery (data not shown). Given the fact that the same PSE-BC promoter-driven GAL4-VP2 expression cassette was inserted into both the single and the separate TSTA Ads, the different protein levels observed imply that a property of the vector genome context or design is influencing GAL4-VP2 expression. We propose in the Discussion that a self-perpetuating feedforward loop may be activated by the head-to-head orientation of AdTSTA-FL. A positive feedback loop could explain the higher basal activity observed for the single virus AdTSTA-FL even in the presence of Casodex (Fig. 5).

DISCUSSION

The key objectives of this study were to investigate the regulation of the TSTA system in different Ad configurations and to define the dynamic range of this system in different *in vivo* settings. Published and ongoing studies by our groups have demonstrated that TSTA technology is an effective approach to augment the activity of a weak tissue-specific promoter [27, 28]. Our goal is to develop these targeted gene expression systems for diagnostic and therapeutic applications in clinical settings. Thus, we have incorporated our PSA promoter-based TSTA system into an adenoviral gene delivery vector. Inserting the two components of TSTA, the activator and the reporter component, into a single vector does improve the functional efficiency of this system *in vivo*. In fact, the activity of the first single vector we generated, AdTSTA-FL, is quite impressive, as its activity consistently exceeded AdCMV-FL in all AR-expressing prostate cancer cell lines and tumors tested ([23] and this study), and it also displayed significant prostate specificity in cell culture studies, achieving 290-fold or higher levels of tissue discrimination (Fig. 2a). AR-mediated expression is a critical component of the PSA-based promoter in the TSTA system. We utilized the optical signal produced by AdTSTA-FL in tumors to monitor the dynamics of AR function during prostate cancer progression [23].

To understand the mechanism of activation of TSTA in adenoviral vectors better, we examined and compared the activity of single and separate TSTA configured Ads. The activity of this TSTA system is fully dependent on the GAL4-VP2 activator (Fig. 6). A second interesting finding is that despite equivalent promoter (PSE-BC) and gene

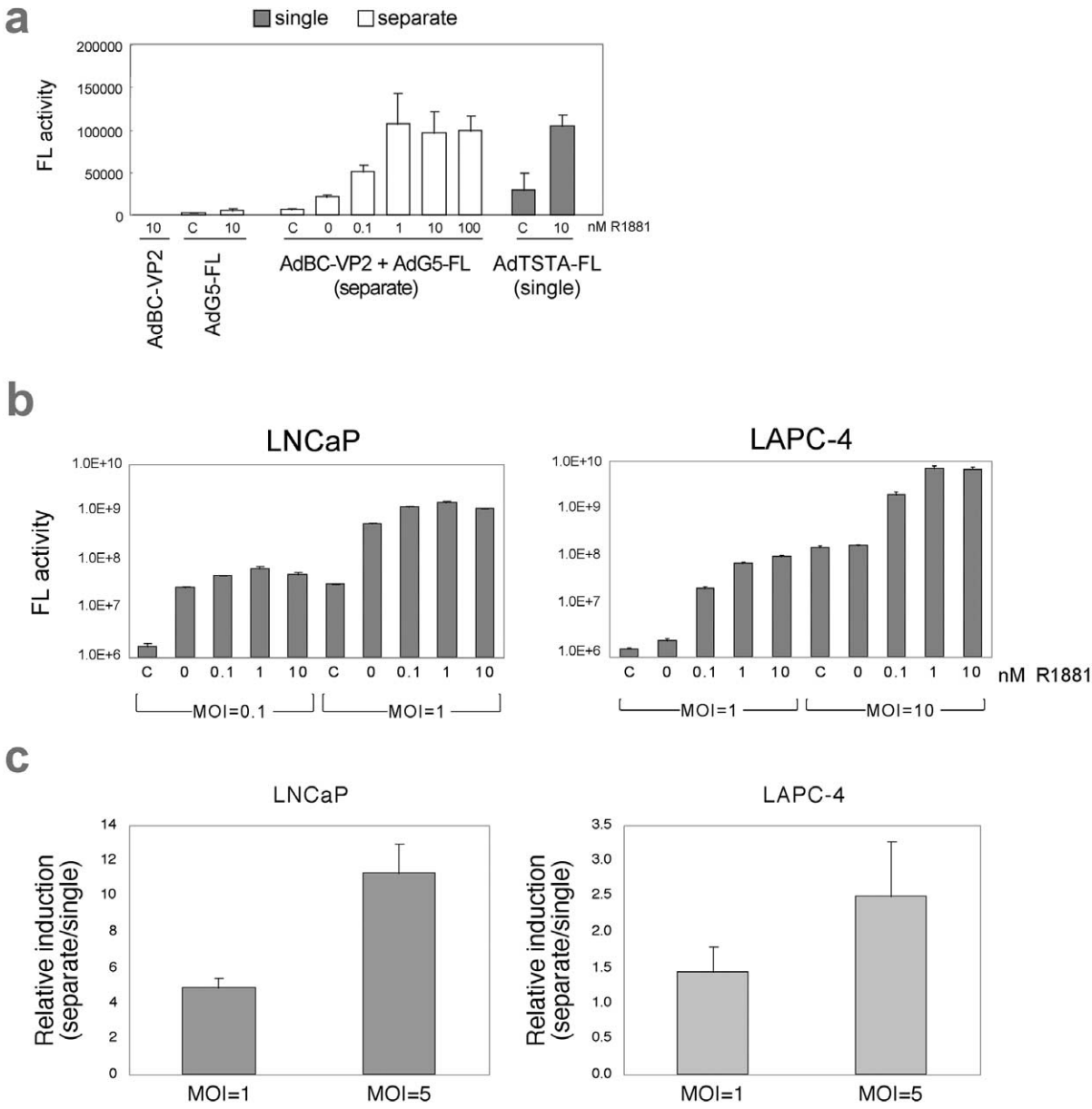

FIG. 5. *In vitro* expression and regulation of the single and separate TSTA Ads. (a) Expression of TSTA Ads in LAPC-4. LAPC-4 cells were infected with Ad at m.o.i. 10. 48 h postinfection the cells were harvested and assayed. Infections with AdBC-VP2 or AdG5-FL exhibited minimal activity. The FL activities of co-infection of separate TSTA Ads increased with increasing amount of synthetic androgen (R1881, nM). C denotes the addition of 10 μM Casodex (anti-androgen). (b) Androgen regulation of AdTSTA-FL. LNCaP and LAPC-4, two androgen-dependent prostate cell lines, were infected with AdTSTA-FL at the indicated m.o.i. in the presence of Casodex or R1881. The FL activities assayed at 48 h postinfection are shown. (c) Relative androgen induction ratio of the separate to the single TSTA Ads. The cells were infected at m.o.i. 1 or 5. Fold induction of activity was calculated based on the ratio of the peak activity (in 10 nM R1881) to the basal activity (in 10 μM Casodex). The relative induction ratio was calculated by dividing the androgen induction in the separate TSTA Ads infection by the induction in the single-AdTSTA-FL-infected cells. The ratio shows that separate TSTA Ads exhibit higher androgen induction than the single Ad.

delivery of the activator in the single and separate TSTA Ads, the single AdTSTA-FL consistently expressed an elevated level of GAL4-VP2 activator. This finding indicates that the head-to-head configuration in the single Ad promotes an increase in GAL4-VP2 and, hence, FL expression. This result could also contribute to the slightly elevated basal activity mediated by AdTSTA-FL in androgen-depleted cell culture medium. We hypothesize that a feedforward loop might be at play in the single AdTSTA-FL. A schematic illustration of this idea is shown in

doi:10.1016/j.ymthe.2003.08.016

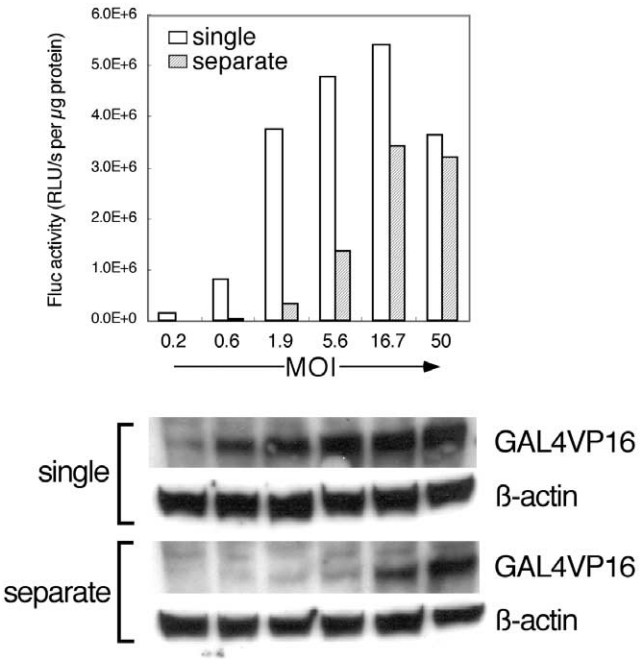

FIG. 6. The activation mechanism in TSTA Ads. LNCaP cells were infected with AdTSTA-FL at specified m.o.i. For the separate system, both AdBC-VP2 and AdG5-FL were infected at the denoted m.o.i. The FL activities and GAL4-VP2 activator expression were examined at 48 h postinfection. Western blot analysis is shown at the bottom. The GAL4-VP2 activator was probed with anti-GAL4 polyclonal antibody (see Materials and Methods). β-Actin is shown as a control.

Fig. 7. The initial expression of GAL4-VP2 (step 1) is regulated by the PSE-BC promoter. In step 2, GAL4-VP2 binds to the GAL4 sites and activates FL gene expression. However, in the head-to-head configuration, the multiple GAL4-VP2 activators could also stimulate transcription in the direction of the PSE-BC promoter in an enhancer-like manner (step 3), further enhancing the synthesis of GAL4-VP2 (step 4). The feedforward loop leads to a perpetuating cycle of activator production that exceeds the natural capability of the PSE-BC promoter. This phenomenon could also contribute to "leaky" expression in nonprostate cells when the TSTA vector is administered at high m.o.i. From these results, we would postulate that functional separation of the activator and reporter components in a single vector might achieve tighter regulation of the TSTA system.

A transcriptionally targeted gene expression approach [reviewed in 45] could reduce the potential side effects of Ad-mediated cytotoxic cancer gene therapy such as that mediated by the herpes simplex virus thymidine kinase (HSV-TK) gene [46]. After intratumoral injection of Ad constitutively expressing luciferase or other reporter gene, leakage of the vector into systemic circulation resulted in transgene expression in the liver [26,47]. From this finding liver toxicity can be anticipated after intratumoral injection of CMV-driven HSV-TK Ad following administration of the prodrug ganciclovir. When a tissue- or cancer-specific promoter is employed to drive HSV-TK, the same extent of vector delivery to the liver is expected to occur. However, HSV-TK expression in the liver will be restricted by the tissue-specific promoter and therefore transgene-mediated liver toxicity should be reduced.

The gene-expression targeting approach employed in this study will not alter the *in vivo* liver distribution observed of Ad5 [26,48]. This preferential Ad transduction has contributed to liver toxicity [48–50] due to the innate immune response to viral capsid proteins [51] and cell-mediated immunity against viral gene products [52,53]. Utilization of a specific promoter to drive transgene expression was shown to reduce both the immune response against the Ad and the associated liver toxicity [54]. In addition, the potent gene expression mediated by the TSTA system could potentially reduce the amount of vector needed to transduce cancer cells *in vivo* compared to nonamplified tissue-specific vectors. Reducing the input dosage of Ad has been documented to reduce liver toxicity [49–52]. A second consequence of Ad sequestration in the liver [48,49] is that viral distribution to other organs such as kidney and intestine was nearly 1000-fold lower [55]. To improve *in vivo* gene transduction to other organs or tumors, many studies are under way to divert the natural adenovirus tropism away from the liver by ablation of CAR- and integrin-mediated interactions [48,55,56].

The inability to detect prostatic expression after tail vein administration of 10^7 pfu of AdTSTA-FL (Figs. 2b and 2c) could be due to liver sequestration. We have detected FL expression in the prostate after intravenous administration of 1.8×10^9 pfu of AdPSE-BC-FL [25]. The AdTSTA-FL is estimated to be about 50-fold more active than AdPSE-BC-FL [23,28]. However, the 180-fold lower dosage of AdTSTA-FL used in this study compared to AdPSE-BC-FL [25] might be below the threshold of detection for

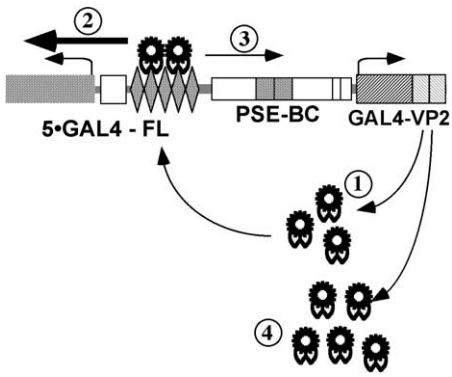

FIG. 7. Schematic representation of the activation mechanism. The feedforward loop mechanism postulates that GAL4-VP2 expression is upregulated by the activator's binding to the designed GAL4 sites in a self-activated manner.

optical imaging. Moreover, by an intraperitoneal route of vector delivery we have been able to detect specific optical signals in the prostate (M. Johnson and L. Wu, unpublished data).

The mechanism for the low level of expression observed in lung tissue is unclear (Figs. 2b and 2c). We speculate that there could be transcription factors common to both lung and prostate that partially contribute to the regulation of the PSA promoter. For example, GATA zinc finger transcription factors have been shown to bind to the PSA promoter [57], and they are involved in lung development [58] and transcription of lung-specific promoters [59]. A large family of Ets transcription factors could also participate in epithelial-specific expression in the lung and prostate [60–62]. Investigating these intriguing possibilities might lead to a better understanding of tissue-specific gene regulation.

It is quite evident that the TSTA approach can amplify the activity of many other weak tissue-specific promoters. Dr. Gambhir's group has demonstrated that the activity of the hypoxia-inducible VEGF promoter can be amplified [63]. A similar approach has been employed to amplify the carcinoembryonic antigen promoter in a binary adenovirus system [64]. This approach exhibited increased therapeutic index compared to constitutive viral RSV-driven HSV-TK suicide gene therapy [64]. To adapt the TSTA system to other promoters, it will be necessary to adjust the various components of TSTA (i.e., the potency of the specific promoter, the strength of the activator, and the number of GAL4 sites) to achieve optimal regulation and expression dictated by the specific applications.

The modular and titratable nature of the TSTA system also makes it particularly attractive for a variety of gene therapy applications [28]. Transgene levels needed to achieve therapeutic efficacy in different gene therapy strategies might vary greatly; for example, p53 tumor suppressor expression in genetic corrective strategies might need to be higher than cytokine expression in immune-mediated tumor rejection. The various adjustable constituents of TSTA can be fine-tuned to achieve the most effective and least toxic therapeutic result. We have shown that transcriptionally targeted Ad (AdPSE-BC-luc) can achieve cell-specific expression to localize metastatic prostate cancer lesions in living mice, using optical CCD imaging [26]. To translate this finding to clinical diagnostic settings, a higher energy imaging modality will be needed to circumvent the loss of optical signal observed with increased tissue depth. Positron emission tomography (PET) is a radionuclide imaging modality widely used in clinical settings. Our institution has acquired substantial experience in adapting this modality to gene-based imaging in small animals, using the HSV-TK or the dopamine type 2 receptor reporter genes [29,30,65]. Compared to optical imaging, PET has the distinct advantage of providing tomographic quantitative image signals and adaptability for human imaging. However, optical imaging is several orders of magnitude higher in sensitivity than PET in small animal applications [66]. Thus, the highly amplified and prostate-specific expression mediated by TSTA will likely permit the development and successful implementation of gene-based PET imaging to detect metastasis *in vivo*.

Many of our studies have demonstrated that the TSTA system is a promising tool to create future targeted gene-based diagnostic and therapeutic applications. With an in-depth understanding of its functional properties and fine-tuning of various components of TSTA, a truly safe, effective, and specific treatment can be developed for metastatic or hormone-refractory prostate cancer.

MATERIALS AND METHODS

Adenovirus constructs. AdCMV-FL was constructed as previously described [25,33]. The single AdTSTA-FL and separate TSTA Ads, AdBC-VP2 and AdG5-FL, were constructed with the AdEasy system [35]. The head-to-head fragment of activator and reporter in the single virus was derived from PBCVP2G5-L [28]. The construction of AdTSTA-FL has been previously described [23]. A *Not*I fragment containing the PSE-BC-driven GAL4-VP2 expression cassette was cloned into the *Not*I site of pShuttle to generate AdBC-VP2. For the construction of AdG5-FL, an *Asp*718–*Sal*I fragment with five GAL4 binding sites upstream of the minimal adenovirus E4 and FL genes was blunted and ligated into the *Eco*RV site of pShuttle. All the pShuttle expression plasmids were used for recombination with pAdEasy-1 in the BJ5183 rec^+ bacteria strain to generate the full-length recombinant virus-containing plasmid. The viruses were propagated in 293 cells, purified on a CsCl gradient, and titered by plaque assays on 293 monolayers. Viruses are stored in 10 mM Tris–HCl, 1 mM $MgCl_2$, and 10% glycerol at −80°C until use.

Cell culture and infection studies. The human prostate cancer cell lines, LNCaP and LAPC-4, were grown in RPMI 1640 and Iscove's modified DMEM, respectively, and supplemented with 10% fetal bovine serum (FBS) and 1% penicillin/streptomycin solution. PC-3, Du145, HeLa, MCF7, HepG2, A549, and H157 cells were cultured in RPMI 1640 (Mediatech, Herndon, VA) with 10% FBS and 1% penicillin/streptomycin. For FL assays, the cultured cells were plated onto 24-well plates at 5×10^4 cells per well, and cells were counted at the day of infection to calculate m.o.i. For prostate cell lines, medium was replaced with 10% charcoal-stripped serum for 2 days prior to infection. The cells were infected with AdTSTA-FL or co-infected with AdBC-VP2 and AdG5-FL at certain m.o.i. Following infection, the synthetic androgen methylenetrienolone (R1881; NEN Life Science Products, Boston, MA) or anti-androgen bicalutamide (Casodex) was added to samples as indicated. At 48 h postinfection, the cells were harvested and lysed, using passive lysis buffer (Promega, Madison, WI). Levels of FL activity were measured according to the manufacturer's instructions (Promega), using a luminometer (Berthold Detection Systems, Pforzheim, Germany) with a 10-s integration time. Each value was calculated as the average of triplicate samples.

Real-time PCR was performed to quantify the amount of intracellular viral DNA. HeLa, MCF7, HepG2, H157, A549, and LNCaP cells were infected with AdG5-FL at m.o.i. 0.1 or 1 36 h after plating. After 12 h, cells were harvested and lysed. The total DNA was prepared with the DNeasy Tissue Kit (Qiagen, Valencia, CA). Opticon2 (MJ Research, Boston, MA) real-time PCR was performed, using these DNAs as template and the DyNAmo SYBR Green qPCR Kit (Finnzymes, Espoo, Finland). The viral FL sequences were detected by the following primer set: FL-a (5′-GAGATACGCCCTGGTTCCTG-3′) and FL-b (5′-GCATACGACGATTCTGTGATTTG-3′). Infectivity was calculated based on the copy number of internalized viral DNA divided by cell number. The relative infectivities of all cells are in reference to HeLa cells, which were set as 1, as they are the least susceptible to infection among the cell lines we tested.

doi:10.1016/j.ymthe.2003.08.016

Animal experiments with CCD imaging. Animal care and procedures were performed in accordance with the University of California Animal Research Committee guidelines. Eight- to ten-week-old male SCID mice (ICRSC-M, ~25 g, Taconic Farms, Germantown, NY) were used in these studies. Human prostate tumor xenografts were generated in SCID mice as previously described [41]. The LAPC-4 xenograft was originally provided by Dr. Charles Sawyers at UCLA. We passaged the tumor by implanting small tumor fragments mixed 1:1 with Matrigel (Collaborative Research, Bedford, MA) subcutaneously into the flanks of male SCID mice.

For the naïve mouse experiments, 10^7 pfu of Ad was injected via the tail vein ($n = 3$). *In vivo* expression was monitored sequentially over time. For the LAPC-4 xenografts, tumors were allowed to grow for 3 weeks prior to injection and reached a diameter of approximately 1 cm. AdBC-VP2 and AdG5-FL (10^8 pfu each) or AdTSTA-FL (10^7 pfu) was injected at three sites on each tumor at 10 μl per site ($n = 3$). Optical CCD imaging was performed at the indicated days postinjection. Intraprostatic injections were performed 7 days after castration. Both castrated and noncastrated animals received injection of 10^8 infectious units each of the paired TSTA Ads or 10^6 infectious units of the single TSTA Ad in both posterior lobes of the prostate ($n = 4$ per group). For each imaging session, the mice were anesthetized with ketamine/xylazine (4:1), and the d-luciferin substrate (150 mg/kg in PBS, Xenogen) was given intraperitoneally at a volume of 200 μl, with a 20-min incubation period prior to imaging. CCD images were obtained using a cooled IVIS CCD camera (Xenogen, Alameda, CA), and images were analyzed with IGOR-PRO Living Image Software, as described [26,28], in units of photons acquired per second per square centimeter per steridan.

Western blot analysis of GAL4-VP2 expression. LNCaP cells were grown in 60-mm dishes and infected with AdTSTA-FL or co-infected with AdBC-VP2 and AdG5-FL at m.o.i. 0.21, 0.62, 1.9, 5.6, 16.7, or 50 (threefold serial dilution). For co-infection, each Ad was administered at the m.o.i. listed above. Forty-eight hours later, the cells were harvested and lysed with RIPA buffer (1% NP-40, 0.1% sodium deoxycholate, 150 mM NaCl, and 50 mM Tris–HCl (pH 7.5), protease inhibitor cocktail (Sigma, St. Louis, MO)). The samples were fractionated on 8–16% gradient acrylamide gels (Gradipore, Frenchs Forest, Australia) and subjected to immunoblot analysis with rabbit polyclonal antibodies generated against intact GAL4-VP2 or β-actin A5316 (Sigma). Detection was done by visualization of bands with HRP-labeled secondary antibody and ECL (Amersham Pharmacia Biotech, Piscataway, NJ).

ACKNOWLEDGMENTS

We appreciate the technical support of Erika Billick, the assistance of Wendy Aft on manuscript preparation, and helpful discussions with Drs. Harvey Herschman and Helen Brown. This work is supported by Department of Defense (DOD) CDMRP PC020536 (to L.W.), California Cancer Research Program 3NI0226 (to L.W.), NIH R01 CA101904 (to L.W.), CapCURE (to M.C., S.S.G.), DOD PC 991019 (to Charles Sawyers and M.C.), DOD PC020177 (to M.C.), an interdisciplinary seed grant from the JCCC (to M.C., L.W., and S.S.G.), R01 CA82214 (to S.S.G.), SAIRP R24 CA92865 (to S.S.G.), and Department of Energy Contract DE-FC03-87ER60615 (to S.S.G.). M.S. is supported by a DOD CDMRP postdoctoral fellowship (PC020531).

RECEIVED FOR PUBLICATION JUNE 16, 2003; ACCEPTED AUGUST 20, 2003.

REFERENCES

1. American Cancer Society (2002). Cancer Facts & Figures 2002. Am. Cancer Soc., Atlanta, pp. 3–15.
2. Denis, L., and Murphy, G. P. (1993). Overview of phase III trials on combined androgen treatment in patients with metastatic prostate cancer. *Cancer* **72:** 3888–3895.
3. Hellerstedt, B. A., and Pienta, K. J. (2002). The current state of hormonal therapy for prostate cancer. *CA Cancer J. Clin.* **52:** 154–179.
4. Labrie, F. (2002). Androgen blockade in prostate cancer in 2002: major benefits on survival in localized disease. *Mol. Cell. Endocrinol.* **198:** 77–87.
5. Mabjeesh, N. J., Zhong, H., and Simons, J. W. (2002). Gene therapy of prostate cancer: current and future directions. *Endocr. Relat. Cancer* **9:** 115–139.
6. Wu, L. and Sato, M. (2003). Integrated, molecular engineering approaches to develop prostate cancer gene therapy. *Curr. Gene Ther.* **3:** 452–467.
7. Cleutjens, K. B., van der Korput, H. A., van Eekelen, C. C., van Rooij, H. C., Faber, P. W., and Trapman, J. (1997). An androgen response element in a far upstream enhancer region is essential for high, androgen-regulated activity of the prostate-specific antigen promoter. *Mol. Endocrinol.* **11:** 148–161.
8. Noss, K. R., Wolfe, S. A., and Grimes, S. R. (2002). Upregulation of prostate specific membrane antigen/folate hydrolase transcription by an enhancer. *Gene* **285:** 247–256.
9. O'Keefe, D. S., *et al.* (1998). Mapping, genomic organization and promoter analysis of the human prostate-specific membrane antigen gene. *Biochim. Biophys. Acta* **1443:** 113–127.
10. Pang, S., *et al.* (1997). Identification of a positive regulatory element responsible for tissue-specific expression of prostate-specific antigen. *Cancer Res.* **57:** 495–499.
11. Schuur, E. R., Henderson, G. A., Kmetec, L. A., Miller, J. D., Lamparski, H. G., and Henderson, D. R. (1996). Prostate-specific antigen expression is regulated by an upstream enhancer. *J. Biol. Chem.* **271:** 7043–7051.
12. Watt, F., *et al.* (2001). A tissue-specific enhancer of the prostate-specific membrane antigen gene, FOLH1. *Genomics* **73:** 243–254.
13. Hobisch, A., Culig, Z., Radmayr, C., Bartsch, G., Klocker, H., and Hittmair, A. (1995). Distant metastases from prostatic carcinoma express androgen receptor protein. *Cancer Res.* **55:** 3068–3072.
14. Koivisto, P. A., and Helin, H. J. (1999). Androgen receptor gene amplification increases tissue PSA protein expression in hormone-refractory prostate carcinoma. *J. Pathol.* **189:** 219–223.
15. Sweat, S. D., Pacelli, A., Bergstralh, E. J., Slezak, J. M., Cheng, L., and Bostwick, D. G. (1999). Androgen receptor expression in prostate cancer lymph node metastases is predictive of outcome after surgery. *J. Urol.* **161:** 1233–1237.
16. van der Kwast, T. H., and Tetu, B. (1996). Androgen receptors in untreated and treated prostatic intraepithelial neoplasia. *Eur. Urol.* **30:** 265–268.
17. Bok, R. A., and Small, E. J. (2002). Bloodborne biomolecular markers in prostate cancer development and progression. *Nat. Rev. Cancer* **2:** 918–926.
18. Feldman, B. J., and Feldman, D. (2001). The development of androgen-independent prostate cancer. *Nat. Rev. Cancer* **1:** 34–45.
19. Visakorpi, T., *et al.* (1995). In vivo amplification of the androgen receptor gene and progression of human prostate cancer. *Nat. Genet.* **9:** 401–406.
20. Gregory, C. W., *et al.* (2001). A mechanism for androgen receptor-mediated prostate cancer recurrence after androgen deprivation therapy. *Cancer Res.* **61:** 4315–4319.
21. Zhou, Z. X., Lane, M. V., Kemppainen, J. A., French, F. S., and Wilson, E. M. (1995). Specificity of ligand-dependent androgen receptor stabilization: receptor domain interactions influence ligand dissociation and receptor stability. *Mol. Endocrinol.* **9:** 208–218.
22. Abreu-Martin, M. T., Chari, A., Palladino, A. A., Craft, N. A., and Sawyers, C. L. (1999). Mitogen-activated protein kinase kinase kinase 1 activates androgen receptor-dependent transcription and apoptosis in prostate cancer. *Mol. Cell. Biol.* **19:** 5143–5154.
23. Zhang, L., *et al.* (2003). Interrogating androgen receptor function in recurrent prostate cancer. *Cancer Res.* **63:** 4552–4560.
24. Latham, J. P., Searle, P. F., Mautner, V., and James, N. D. (2000). Prostate-specific antigen promoter/enhancer driven gene therapy for prostate cancer: construction and testing of a tissue-specific adenovirus vector. *Cancer Res.* **60:** 334–341.
25. Wu, L., *et al.* (2001). Chimeric PSA enhancers exhibit augmented activity in prostate cancer gene therapy vectors. *Gene Ther.* **8:** 1416–1426.
26. Adams, J. Y., *et al.* (2002). Visualization of advanced human prostate cancer lesions in living mice by a targeted gene transfer vector and optical imaging. *Nat. Med.* **8:** 891–897.
27. Iyer, M., Wu, L., Carey, M., Wang, Y., Smallwood, A., and Gambhir, S. S. (2001). Two-step transcriptional amplification as a method for imaging reporter gene expression using weak promoters. *Proc. Natl. Acad. Sci. USA* **98:** 14595–14600.
28. Zhang, L., *et al.* (2002). Molecular engineering of a two-step transcription amplification (TSTA) system for transgene delivery in prostate cancer. *Mol. Ther.* **5:** 223–232.
29. Blasberg, R. G., and Tjuvajev, J. G. (1999). Herpes simplex virus thymidine kinase as a marker/reporter gene for PET imaging of gene therapy. *Q. J. Nucl. Med.* **43:** 163–169.
30. Gambhir, S. S. (2002). Molecular imaging of cancer with positron emission tomography. *Nat. Rev. Cancer* **2:** 683–693.
31. Massoud, T., and Gambhir, S. S. (2003). Molecular imaging in living subjects: seeing fundamental biological processes in a new light. *Genes Dev.* **17:** 545–580.
32. Rehemtulla, A., *et al.* (2000). Rapid and quantitative assessment of cancer treatment response using in vivo bioluminescence imaging. *Neoplasia* **2:** 491–495.
33. Wu, J. C., Sundaresan, G., Iyer, M., and Gambhir, S. S. (2001). Noninvasive optical imaging of firefly luciferase reporter gene expression in skeletal muscles of living mice. *Mol. Ther.* **4:** 297–306.
34. Ciana, P., *et al.* (2003). In vivo imaging of transcriptionally active estrogen receptors. *Nat. Med.* **9:** 82–86.
35. He, T. C., Zhou, S., da Costa, L. T., Yu, J., Kinzler, K. W., and Vogelstein, B. (1998). A simplified system for generating recombinant adenoviruses. *Proc. Natl. Acad. Sci. USA* **95:** 2509–2514.
36. Bergelson, J. M., *et al.* (1997). Isolation of a common receptor for coxsackie B viruses and adenoviruses 2 and 5. *Science* **275:** 1320–1323.
37. Roelvink, P. W., Mi Lee, G., Einfeld, D. A., Kovesdi, I., and Wickham, T. J. (1999).

Identification of a conserved receptor-binding site on the fiber proteins of CAR-recognizing adenoviridae. *Science* **286:** 1568–1571.
38. Wickham, T. J., Mathias, P., Cheresh, D. A., and Nemerow, G. R. (1993). Integrins alpha v beta 3 and alpha v beta 5 promote adenovirus internalization but not virus attachment. *Cell* **73:** 309–319.
39. Fechner, H., *et al.* (2000). Trans-complementation of vector replication versus coxsackie–adenovirus-receptor overexpression to improve transgene expression in poorly permissive cancer cells. *Gene Ther.* **7:** 1954–1968.
40. Rauen, K. A., *et al.* (2002). Expression of the coxsackie adenovirus receptor in normal prostate and in primary and metastatic prostate carcinoma: potential relevance to gene therapy. *Cancer Res.* **62:** 3812–3818.
41. Klein, K. A., *et al.* (1997). Progression of metastatic human prostate cancer to androgen independence in immunodeficient SCID mice. *Nat. Med.* **3:** 402–408.
42. Fechner, H., *et al.* (1999). Expression of coxsackie adenovirus receptor and alphav-integrin does not correlate with adenovector targeting in vivo indicating anatomical vector barriers. *Gene Ther.* **6:** 1520–1535.
43. Kijima, T., *et al.* (1999). Application of the Cre recombinase/loxP system further enhances antitumor effects in cell type-specific gene therapy against carcinoembryonic antigen-producing cancer. *Cancer Res.* **59:** 4906–4911.
44. Ueda, K., *et al.* (2001). Carcinoembryonic antigen-specific suicide gene therapy of cytosine deaminase/5-fluorocytosine enhanced by the Cre/loxP system in the orthotopic gastric carcinoma model. *Cancer Res.* **61:** 6158–6162.
45. Wu, L., Johnson, M. and Sato, M. (2003). Transcriptionally-targeted gene therapy to detect and treat cancer. *Trends Mol. Med.* **9:** 421–429.
46. Shalev, M., *et al.* (2000). Suicide gene therapy toxicity after multiple and repeat injections in patients with localized prostate cancer. *J. Urol.* **163:** 1747–1750.
47. Lohr, F., Huang, Q., Hu, K., Dewhirst, M. W., and Li, C. Y. (2001). Systemic vector leakage and transgene expression by intratumorally injected recombinant adenovirus vectors. *Clin. Cancer Res.* **7:** 3625–3628.
48. Alemany, R., and Curiel, D. T. (2001). CAR-binding ablation does not change biodistribution and toxicity of adenoviral vectors. *Gene Ther.* **8:** 1347–1353.
49. Tao, N., *et al.* (2001). Sequestration of adenoviral vector by Kupffer cells leads to a nonlinear dose response of transduction in liver. *Mol. Ther.* **3:** 28–35.
50. Morral, N., *et al.* (2002). Lethal toxicity, severe endothelial injury, and a threshold effect with high doses of an adenoviral vector in baboons. *Hum. Gene Ther.* **13:** 143–154.
51. Zhang, Y., *et al.* (2001). Acute cytokine response to systemic adenoviral vectors in mice is mediated by dendritic cells and macrophages. *Mol. Ther.* **3:** 697–707.
52. Yang, Y., Su, Q., and Wilson, J. M. (1996). Role of viral antigens in destructive cellular immune responses to adenovirus vector-transduced cells in mouse lungs. *J. Virol.* **70:** 7209–7212.
53. Jooss, K., Yang, Y., Fisher, K. J., and Wilson, J. M. (1998). Transduction of dendritic cells by DNA viral vectors directs the immune response to transgene products in muscle fibers. *J. Virol.* **72:** 4212–4223.
54. Pastore, L., *et al.* (1999). Use of a liver-specific promoter reduces immune response to the transgene in Ads. *Hum. Gene Ther.* **10:** 1773–1781.
55. Nakamura, T., Sato, K., and Hamada, H. (2003). Reduction of natural adenovirus tropism to the liver by both ablation of fiber-coxsackievirus and adenovirus receptor interaction and use of replaceable short fiber. *J. Virol.* **77:** 2512–2521.
56. Einfeld, D. A., *et al.* (2001). Reducing the native tropism of adenovirus vectors requires removal of both CAR and integrin interactions. *J. Virol.* **75:** 11284–11291.
57. Perez-Stable, C. M., Pozas, A., and Roos, B. A. (2000). A role for GATA transcription factors in the androgen regulation of the prostate-specific antigen gene enhancer. *Mol. Cell. Endocrinol.* **167:** 43–53.
58. Laverriere, A. C., MacNeill, C., Mueller, C., Poelmann, R. E., Burch, J. B., and Evans, T. (1994). GATA-4/5/6, a subfamily of three transcription factors transcribed in developing heart and gut. *J. Biol. Chem.* **269:** 23177–23184.
59. Bruno, M. D., Korfhagen, T. R., Liu, C., Morrisey, E. E., and Whitsett, J. A. (2000). GATA-6 activates transcription of surfactant protein A. *J. Biol. Chem.* **275:** 1043–1049.
60. Neve, R., *et al.* (1998). The epithelium-specific ets transcription factor ESX is associated with mammary gland development and involution. *FASEB J.* **12:** 1541–1550.
61. Oettgen, P., *et al.* (2000). PDEF, a novel prostate epithelium-specific ets transcription factor, interacts with the androgen receptor and activates prostate-specific antigen gene expression. *J. Biol. Chem.* **275:** 1216–1225.
62. Tymms, M. J., *et al.* (1997). A novel epithelial-expressed ETS gene, ELF3: human and murine cDNA sequences, murine genomic organization, human mapping to 1q32.2 and expression in tissues and cancer. *Oncogene* **15:** 2449–2462.
63. Wang, Y., Iyer, M., Wu, L., Carey, M., and Gambhir, S. S. (2002). A two-step transcriptional approach for imaging of vascular endothelial growth factor (VEGF) gene expression using a bioluminescent reporter gene. *Mol. Imaging Biol.* **4:** S42.
64. Qiao, J., *et al.* (2002). Tumor-specific transcriptional targeting of suicide gene therapy. *Gene Ther.* **9:** 168–175.
65. Gambhir, S. S., *et al.* (2000). Imaging transgene expression with radionuclide imaging technologies. *Neoplasia* **2:** 118–138.
66. Ray, P., Wu, A. M., and Gambhir, S. S. (2003). Optical bioluminescence and positron emission tomography imaging of a novel fusion reporter gene in tumor xenografts of living mice. *Cancer Res.* **63:** 1160–1165.